Available online at www.sciencedirect.com
ScienceDirect
Energy Procedia 83 (2015) 341 – 349
Energy Procedia

7th International Conference on Sustainability in Energy and Buildings

Numerical investigation of counter flow plate heat exchanger

Václav Dvořák[a]*, Tomáš Vít[a]

[a]Technical University of Liberec, Studentska 2, Liberec, 46117, Czech Republic

Abstract

Flow and heat transfer in a recuperative counter flow plate air-to-air heat exchanger were investigated numerically using Fluent software. It was employed previously developed methods to generate a computational mesh and assumed a zero thickness of the plates to calculate the flow in an air-to-air heat exchanger. Pressure loss and effectiveness were evaluated as functions of inner velocity. Obtained numerical data were substituted by suggested functions dependent on the Reynolds number. A function for the loss coefficient was based on the presumption that losses consist of local losses and friction losses. The function for the Nusselt number used the ordinary power function of the Reynolds number for forced convection. The effect of material thickness on pressure loss and effectiveness was illustrated. Even a very thin material for the plate significantly affects pressure loss, while the effect on the effectiveness depended on the thermal conductivity of plate material used. From this results, it is obvious that a thin as possible material is crucial for creating the most effective recuperative air-to-air heat exchanger with high effectiveness and low pressure loss, while the properties of the material itself are unimportant. We compared numerical data with data obtained by measuring a real heat exchanger. The results for effectiveness corresponded well and corrections made were negligible. The results for pressure loss differed significantly, but this difference was lowered by correcting for plate thickness.

Peer-review under responsibility of KES International

Keywords: Heat exchanger, CFD;

1. Introduction

Energy recovery is one of the ways to reduce the energy consumption of buildings. The main component of any energy recovery devices are heat exchangers. Development of recuperative heat exchangers in recent years has focused on increasing their effectiveness. Another challenge is the development of so-called enthalpy exchangers for

* Corresponding author. Tel.: +420485353479.
Email address: vaclav.dvorak@tul.cz

Peer-review under responsibility of KES International
doi:10.1016/j.egypro.2015.12.188

simultaneous heat and moisture transport, i.e. transport of both sensible and latent heat, as presented by Vít et al. in work [1]. To develop heat exchangers, methods of computational fluid dynamics are increasingly used, but there are still some problems to transmit the calculation results to the manufacturing process.

Nomenclature

A	area of heat exchange surface (m^2)
c_p	isobaric specific heat capacity ($J\ kg^{-1}\ K^{-1}$)
C	coefficient in
C_f	correction for friction coefficient (1)
d	gap between plates, channel high (m)
f	friction coefficient (1)
L	length of the heat exchanger (m)
$\dot{m}$	mass flow rate ($kg\ s^{-1}$)
n	exponent in criterial equation for Nusselt number (1)
Nu	Nusselt number (1)
v	velocity ($m\ s^{-1}$)
p	pressure (Pa)
Re	Reynolds number (1)
t	temperature (°C)
s	plate pitch (m)
U	overall heat transfer coefficient ($W\ m^{-2}\ K^{-1}$)
δ	plate thickness (m)
Δ	difference (-)
λ_f	thermal conductivity of fluid – air ($W\ m^{-1}\ K^{-1}$)
λ	thermal conductivity of plate material ($W\ m^{-1}\ K^{-1}$)
ν	kinematic viscosity of air ($m^2\ s^{-1}$)
ρ	density ($kg\ m^{-3}$)
η	effectiveness of heat recovery (1)
ξ_F	final loss coefficient of the heat exchanger (1)
ξ_S	local loss coefficient of the heat exchanger (1)

To simulate a heat exchanger, it is necessary to create a model and a computational mesh and then use computational fluid dynamic (CFD) software. When assembling the heat exchanger, complicated and irregular narrow channels are created. These channels are split into small volumes (elements). The final meshes are structured or unstructured with different element sizes. Several other researchers have dealt with the design of plate heat exchangers and have investigated the performance and loss of pressure of exchangers using numerical simulations. Most of them used an unstructured mesh for their calculations.

Gherasim et al., in work [2], presented a comparison of various grids for a plate heat exchanger modeled by a tetrahedral mesh. In order to assess the influence of the grid resolution on the solution, five grids were created and tested by meshing the volumes with different interval sizes. Laminar and turbulent regimes were simulated. The evolution of the average pressure and average temperature of the hot fluid over transversal sections along the length of the plate was investigated. In general, the differences between the series for the turbulent case were larger than those for the laminar case. It was discovered that the two grids with the smallest elements provided very similar results. In terms of temperature, the obtained results were close for grids with smaller elements. For pressure, quite a large difference between the grid with smallest elements and the grid with the largest ones was discovered.

Subsequent researchers have used numerical simulations to investigate plate heat exchangers with chevron (undulated) profiles. Tsai [3] and Liu [4], for example, dealt with these heat exchangers and their different geometries. Their conclusions regarding temperature and pressure loss were similar to Gherasim [2].

Novosád, in work [5], investigated the influence of oblique waves on the heat transfer surface. The main difficulty faced in this work was the creation of custom geometry. Each version had to be modeled separately and meshed. Each model had to be loaded into the solver, the boundary conditions set, and subsequently evaluated by calculation.

The disadvantages of the repeated generation of computational meshes are: It is slow, meshes made in different models are not similar, and parameterization of the model is problematic. Further, even a small change of geometry requires the whole process of model creation and mesh generation to be gone through again. As a result, there is a high probability of introducing errors into the model and obtaining a low quality of mesh cells. It is necessary to setup the solver, boundary conditions, and all models for all computed variants. Furthermore, meshes are not similar, i.e. the size, shape, and height of cells adjacent to walls are not the same for different topologies.

Therefore, Dvořák, in works [6] and [7], developed a new method for generating computational variants. This method was based on a dynamic mesh, which is provided by Fluent software. The meshes were created by pulling, which is similar to the own production process, i.e. it the pulling direction is perpendicular to the plates. The main advantage is that this type of variant generation is automatic and controlled by in-house software. All computational variants thus have a similar mesh.

Furthermore, Dvořák and Novosád, in work [8], investigated the influence of mesh quality and density on the numerical calculation of a heat exchanger with undulations in a herringbone pattern. They compared the results of the numerical calculation obtained for unstructured meshes made manually with structured but deformed meshes and examined the effect of computational cell size and the number of layers of computational cells across half of the channel. They found that very coarse meshes can yield both too high and unrealistic effectiveness and pressure loss compared to other results. It seems that for deformed meshes, which are structured, the appropriate element size is 0.7 mm, although this size is sometimes not suitable for unstructured meshes.

The aim of this work was to calculate a real counter flow heat exchanger and to compare numerical results with experimental.

2. Methods

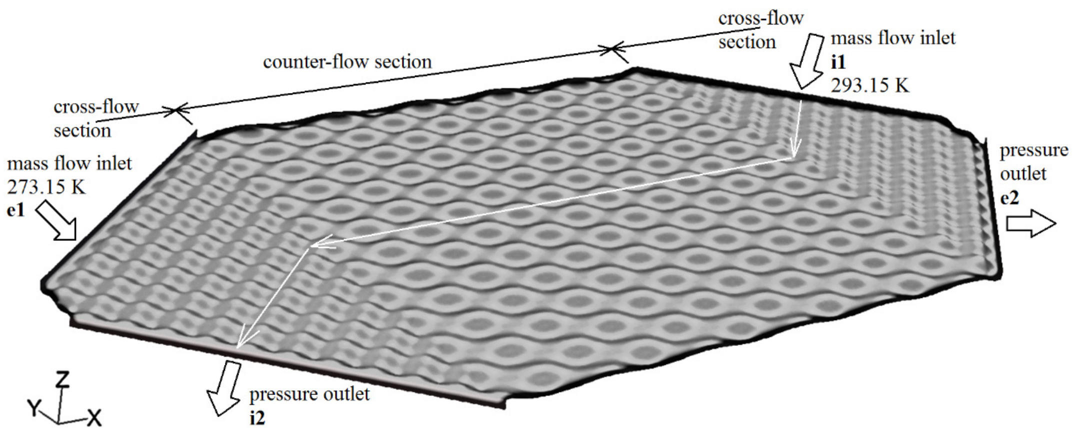

Fig. 1. Schema of a plate heat exchanger model and boundary conditions.

The schema of the numerical model of the plate heat exchanger is shown in Fig. 1. The plate heat exchanger had a typical shape, with inlet cross-flow sections in a triangular shape, which served to distribute the airflow across the heat exchanger before it entered the counter-flow section in the middle of the exchanger. The white line in Fig. 1 represents the ideal path along which the air flowed. Due to the way the plate heat exchanger was assembled, we calculated the flow and heat transfer around two plates. A periodical boundary condition was applied on the upper and the lower boundary conditions, which were parallel to the heat exchanger plates.

We employed a previously developed method to create the computational mesh and to shape the plates of the heat exchanger, see works [6, 7]. The proper density of the mesh was subsequently confirmed in work [8]. An incompressible fluid (air), with properties independent of temperature, was used: thermal conductivity $\lambda_f = 0.0242$ (W m^{-1} K^{-1}), kinematic viscosity $\nu = 17.894 \cdot 10^{-6}$ (m^2 s^{-1}), and density $\rho = 1.225$ (kg m^{-3}). We used mass flow inlets as inlet boundary conditions with specified temperatures of 0 and 20°C, as well as various mass flow rates, to obtain the characteristics of the heat exchanger. Outlet boundary conditions were specified by static pressure.

The two main properties of recuperative heat exchangers used in HVAC systems are the coefficient of effectiveness and pressure loss. Both are dependent on the mass flow rate of air and are evaluated from numerical data. The coefficient of effectiveness (or effectiveness) is an efficiency of the transfer of sensible heat. Most recuperative heat exchangers in air conditioning systems work in isobaric mode, where mass flow rates of warm and cold air are equal, i.e. $\dot{m}_e = \dot{m}_i$. Assuming parity between specific heat capacities, $c_{pe} = c_{pi}$, we can write the effectiveness as

$$\eta = \frac{T_{e2} - T_{e1}}{\Delta t} = \frac{T_{e2} - T_{e1}}{T_{i1} - T_{e1}} = \frac{T_{i1} - T_{i2}}{T_{i1} - T_{e1}} \quad , \tag{1}$$

where $T_{i1} = 293.15$ (K) is the inlet temperature of internal air, $T_{e1} = 273.15$ (K) is the inlet temperature of external air, and T_{e2} (K) is the outlet temperature of external air. The coefficient of effectiveness obtained by numerical calculation as a function of mass flow rate is shown in Fig. 2a.

The difference in total pressure loss between the inlet and outlet was used to assess a drop in pressure

$$\Delta p = \bar{p}_{01} - \bar{p}_{02} \quad , \tag{2}$$

where $\bar{p}_{01}$ (Pa) is the mass-averaged total pressure in the inlet and $\bar{p}_{02}$ (Pa) is the mass-averaged total pressure in the pressure outlet. Pressure drop as a function of the mass flow rate, which was obtained by numerical calculation, is shown in Fig. 2b.

3. Results

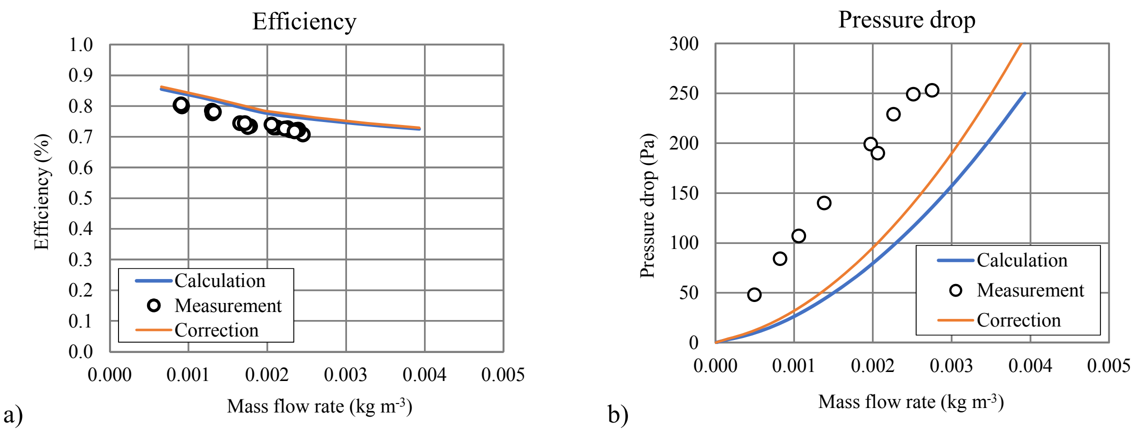

Fig. 2. (a) Effectiveness as a function of mass flow rate; (b) Pressure drop as a function of mass flow rate.

As can be seen from Fig. 2, the effectiveness decreased at a higher mass flow rate, while the drop in pressure increased. We can also see that there was relatively good agreement among numerical results; the calculation overestimated the effectiveness obtained by measurement by 3%. The differences between the calculated and measured pressure drop was bigger; the calculation underestimated the pressure drop by 75% for the lowest mass flow rate and by 19% for the highest.

The differences can be explained by assuming a zero thickness of the material of the heat exchanger plates and neglecting heat resistance of the plates. To correct our numerical results, it was necessary to take the influence of the plate thickness into account.

To better understand these trends and to allow further analysis, we substituted the obtained data with suitable functions.

We expected pressure losses, which were responsible for a drop in pressure, to consist of friction losses and local losses. Due to the low Reynolds number, we assumed a dominant laminar flow. Therefore, we assumed the following form of pressure loss

$$\Delta p_0 = \rho \frac{v^2}{2}\left(\xi_S + \frac{L}{2d} f\right), \tag{3}$$

where d (m) is the gap between the plates of the heat exchanger, L (m) is the length of the heat exchanger or the length of the path the air flows through, f (1) is the friction coefficient, and ξ_S (1) is the sum of the coefficients of local losses, which is obtained from numerical results. For our case we obtained $\xi_S = 24.1$. For laminar flow, we assumed the friction coefficient to be directly dependent on the Reynolds number by equation

$$f = \frac{64}{\mathrm{Re}}, \tag{4}$$

by introducing the definition of Re into equation (3) and dividing it by dynamic pressure $\rho v^2/2$ we arrived at the following form of the final coefficient of pressure losses

$$\xi_F = \left(\xi_S + \frac{L}{d}\frac{32}{\mathrm{Re}} C_\lambda\right) \quad , \tag{5}$$

where C_f (1) is the correction for the friction coefficient obtained from the numerical results. In our case, we obtained $C_f = 2.24$. This quite high value is was caused by the flow in the so-called inlet cross-flow sections of the heat exchanger, where the velocity was higher than in the counter-flow section. The dependence of the loss coefficient on the Reynolds number is shown in Fig. 3a. As can be seen, the suggested equation (5) can easily substitute for the obtained numerical data.

For evaluating heat transfer, we assumed a dependence of the Nusselt number on the Reynolds number

$$\mathrm{Nu} = C\mathrm{Re}^n, \tag{6}$$

where the constants evaluated from the results were $C = 0.4316$ and $n = 0.5367$. Prandt number is considered to be constant for air in the expected temperature range and is included in the constant C. Comparison of the numerical calculation and a substitution with equation (6) is shown in Fig. 3b. Again, the suggested equation substituted easily for original data.

As stated above, the numerical results were obtained for a zero thickness of the material of the heat exchanger due to several reasons. First, it was easier to model the heat exchanger without any real thickness of the plates. Second, the heat transfer from one air to the second one is mainly influenced by the heat transfer from the air to the walls, while the conduction through the plates is usually negligible. It is due to the higher heat resistance of the boundary layers compared to heat resistance of the thin plates, which are usually about 0.1 (mm) thick. The third reason for using plates with zero thickness was that the final thickness of the heat exchanger was not known.

Manufacturers of recuperative heat exchangers for HVAC systems consider the whole cross section of the heat exchanger without considering the thickness of the plates. Therefore, it was necessary to adjust the obtained numerical data according to the actual thickness of the heat exchanger plates.

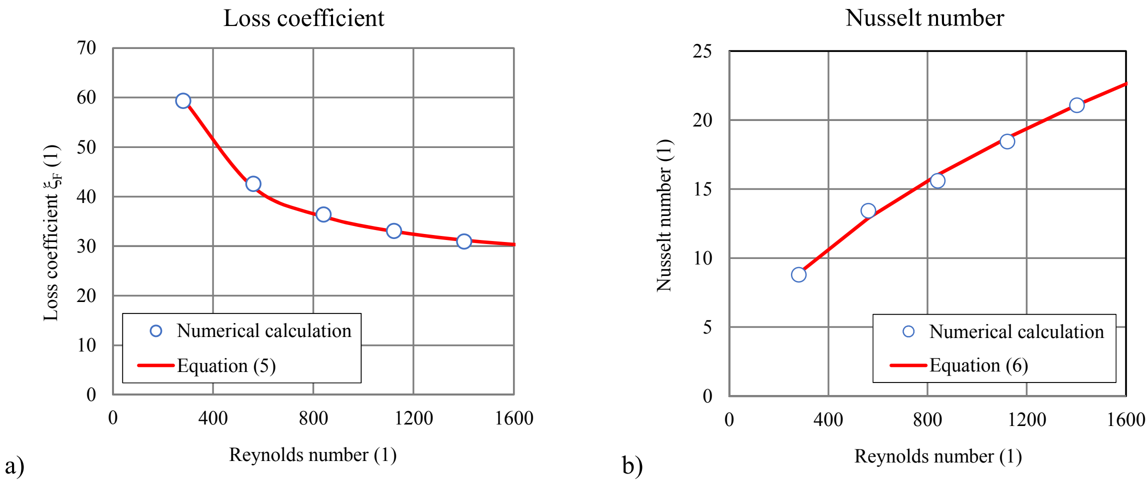

Fig. 3. (a) Loss coefficient evaluated from the numerical results as a function of the Reynolds number; (b) Nusselt number evaluated from the numerical results as a function of the Reynolds number.

To do this, the previously introduced equations were used. We also assumed that these characteristics did not change for a non-zero thickness of the material of the heat exchanger. The real space between plates is given by this difference

$$d = s - \delta, \tag{7}$$

where s (m) is the plate pitch and δ (m) is the plate thickness. Similarly, the characteristic dimension $2d$ will decrease. For a non-zero thickness and for a given mass flow rate of air through the heat exchanger, the velocity increases according to the reciprocal value, yet the Reynolds number remains the same, i.e. $\mathrm{Re}' = \mathrm{Re}$. To calculate the loss coefficient of the heat exchanger, we simply introduced the correct space t into equation (5), but it was necessary to consider the different dynamic pressures. Then, the equation (5) turns into the following form

$$\xi_F' = \left(\frac{s}{s-\delta}\right)^2 \left(\xi_S + \frac{L}{s-\delta}\frac{32}{\mathrm{Re}} C_\lambda\right). \tag{8}$$

The dependence of pressure losses due to a non-zero material thickness is plotted in Fig. 4a. The ratio of ξ_F'/ξ_F is a function of ratio δ/s and Re in the diagram. As can be seen, even with a very minimal thickness of the material and a ratio of $\delta/s = 0.05$, the pressure losses increased by (12 ÷ 13)%. For extremely thick material, e.g. $\delta/s = 0.25$, the drop in pressure reached 100% and was higher for lower Reynolds numbers.

The influence of material thickness on heat transfer is more complex. The Nusselt number remains unchanged because it is dependent only on the Reynolds number, which does not change with material thickness. However, the heat transfer convection changes due to a change in the characteristic dimension. The material thickness also affects thermal conduction in the material itself. The overall heat transfer coefficient in the presented heat exchanger configuration was given by equation

$$U = \frac{1}{\dfrac{4(s-\delta)}{Nu\,\lambda_f} + \dfrac{\delta}{\lambda}}, \tag{9}$$

where λ_f (W m^{-1} K^{-1}) is the thermal conductivity of air and λ (W m^{-1} K^{-1}) is the thermal conductivity of the plate material. To calculate the effect of the change in heat passage on the total transferred heat in the heat exchanger, it was also necessary to take into account the change of the temperature gradient across the heat exchanger. Assuming the same flow rates and constant value of specific heat in both streams the heat balance can be expressed as

$$\dot{m} c_p \Delta T\, \eta = U\, A \Delta T\, (1-\eta), \tag{10}$$

where $\dot{m}$ (kg s^{-1}) is the mass flow rate of the air, c_p is the specific heat capacity (J kg^{-1} K^{-1}), A (m^2) is the area of heat exchange surface, and ΔT (K) is the highest temperature difference. The left side of the equation represents heat flux obtained by one air stream and given by the second air stream. The right side of the equation represents heat flux through the plates. By rearranging equation (10), we get the following formula for effectiveness

$$\eta = \frac{UA}{\dot{m} c_p + UA}. \tag{11}$$

As estimated from formula (11), the effectiveness will be higher for lower mass flow rates and for higher coefficients U. The effect of material thickness and thermal conductivity is plotted in Fig. 4b. As can be seen, for a thermal conductivity of plate material higher than $\lambda = 0.09$ W m^{-1} K^{-1}, the effect of material thickness on effectiveness was positive, but an additional rise in effectiveness was minimal for $\lambda > 0.2$ W m^{-1} K^{-1} and became negligible for $\lambda > 1$ W m^{-1} K^{-1}. On the other hand, for low thermal conductivity, i.e. $\lambda < 0.09$ W m^{-1} K^{-1}, the effect of material thickness was negative because the thermal resistance of the plates became relevant.

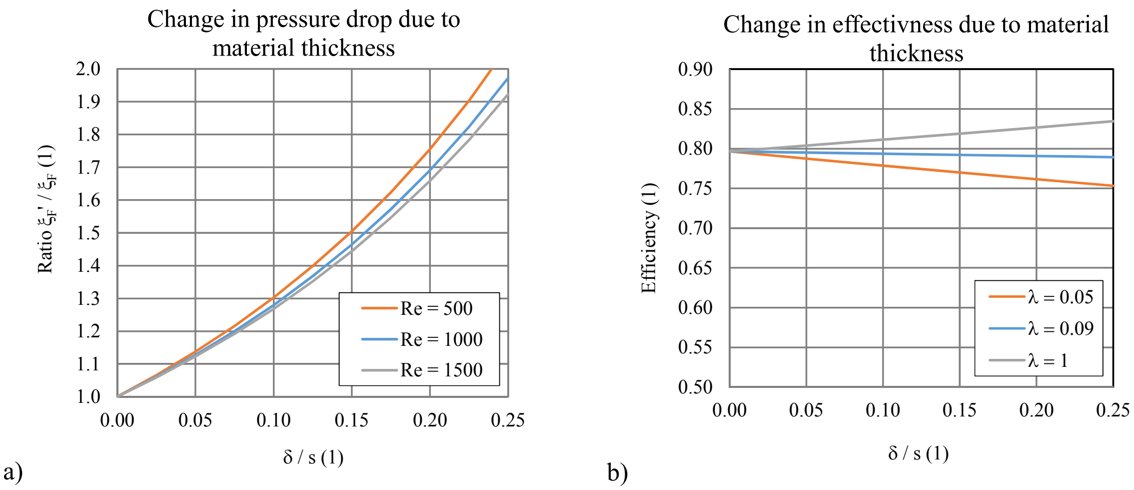

Fig. 4. (a) Change in losses due to material thickness as a function of the ratio δ/s and the Reynolds number; (b) Change in effectiveness due to material thickness as a function of the ratio δ/s and thermal conductivity λ (W m^{-1} K^{-1}).

The results of the corrections for our case are shown in Fig. 1. We can see that a correction that took plate thickness and thermal conductivity into account yielded an even higher effectiveness than effectiveness obtained by calculations. The overall correction increased the calculated effectiveness by 0.9%. The influence of plate thickness on pressure drop was more significant, and in our case, the correction increased the calculated pressure drop by 24%. However, the measured pressure drop was still distinctly higher. This high difference in pressure drop can be explained by several effects that were not taken into account during the calculations: the effect of plate roughness, the effect of plate deformation, and the effect of other imperfections and differences between the shapes of the numerical model and the real plates of the heat exchangers.

4. Conclusion

Flow and heat transfer in a recuperative counter flow plate heat exchanger were investigated numerically using Fluent software. We employed previously developed methods to generate a computational mesh and assumed a zero thickness of the plates to calculate the flow in an air-to-air heat exchanger. Pressure loss and effectiveness were evaluated as functions of inner velocity. Obtained numerical data were substituted by suggested functions dependent on the Reynolds number. A function for the loss coefficient was based on the presumption that losses consist of local losses and friction losses. The function for the Nusselt number used the ordinary power function of the Reynolds number for forced convection.

We used these functions to illustrate the effect of material thickness on pressure loss and effectiveness. We discovered that even a very thin material for the plate significantly affects pressure loss, e.g. if the thickness of the material was only 5% of the plate pitch, the pressure losses were increased by at least 12% compared to a zero thickness and was higher for lower Reynolds numbers. The effect of plate thickness on the effectiveness depended on the thermal conductivity of plate material used. If the thermal conductivity coefficient was $\lambda < 0.09$ W m^{-1} K^{-1}, the effectiveness decreased with plate thickness because the thermal conductivity became relevant. If $\lambda > 0.09$ W m^{-1} K^{-1}, the effectiveness even increased with plate thickness, but any additional rise in effectiveness became negligible for $\lambda > 1$ W m^{-1} K^{-1}. From this results, it is obvious that a thin as possible material is crucial for creating the most effective recuperative air-to-air heat exchanger with high effectiveness and low pressure loss, while the properties of the material itself are unimportant.

We compared numerical data with data obtained by measuring a real heat exchanger. The results for effectiveness corresponded well; the calculations overestimated measured effectiveness by 3% and corrections made were negligible. The results for pressure loss differed significantly; the calculation underestimated the measured pressure drop by (19 ÷ 75)%, but this difference was lowered by correcting for plate thickness. This high difference in pressure loss can be explained by several effects that were not taken into account during calculations: the effect of plate roughness, the effect of plate deformation, and the effect of other imperfections and differences between the shapes of the numerical model and the real plates of the heat exchangers.

Acknowledgements

The author gratefully acknowledges the financial support from the Czech Technological Agency under project TACR TA01020313.

References

[1] Vít T, Novotný P, Nguyen V, Dvořák V. Testing method of materials for enthalpy wheels. Recent Advances in Energy, Environment, Economics and Technological Innovation, Paris, France, 29th – 31st October; 2013.

[2] Gherasim I, Galanis N., Nguyen CT. Heat transfer and fluid flow in a plate heat exchanger. Part II: Assessment of laminar and two-equation turbulent models. International Journal of Thermal Sciences 50; 2011. p. 1499-1511

[3] Tsai YCh, Liu FB, Shen, P T. Investigation of effect of oblique ridges on heat transfer in plate heat exchangers. International Communications in Heat and Mass Transfer 36; 2009. p. 574–578

[4] Liu FB, Tsai YCh. An experimental and numerical investigation of fluid flow in a cross-corrugated channel. Heat Mass Transfer 46; 2010. p. 585–593

[5] Novosád J, Dvořák V. Investigation of effect of oblique ridges on heat transfer in plate heat exchangers. Experimental Fluid Mechanics 2013, November 19.-22.; 2013. p. 510 - 514

[6] Dvořák V. A method for optimization of plate heat exchanger. 18th International Conference on Circuits, Systems, Communications and Computers, Santorini Island, Greece, July 17-21; 2014.

[7] Dvořák V. Optimization of plate heat exchangers with angled undulations in herringbone pattern. The 7th International Meeting on Advances in Thermofluids, Kuala Lumpur, Malaysia, November, 26-27; 2014.

[8] Dvořák V, Novosad J. Influence of mesh quality and density on numerical calculation of heat exchanger with undulation in herringbone pattern. 19th International Conference on Circuits, Systems, Communications and Computers, Zakynthos, Greece, July 16-20; 2015 (submitted).